

Electronic shell study of prolate Li_n (n =15-17) clusters: Magnetic superatomic molecules

Lijuan Yan(闫丽娟)†, Jianmei Shao(邵健梅), and Yongqiang Li(李永强)\cclink

Citation: Chin. Phys. B, 2020, 29 (**12**): 125101. DOI: 10.1088/1674-1056/abb669

Journal homepage: http://cpb.iphy.ac.cn; http://iopscience.iop.org/cpb

What follows is a list of articles you may be interested in

Theoretical insights into photochemical ESITP process for novel DMP-HBT-py compound

Guang Yang(杨光), Kaifeng Chen(陈凯锋), Gang Wang(王岗), Dapeng Yang(杨大鹏)

Chin. Phys. B, 2020, 29 (**10**): 103103. DOI: 10.1088/1674-1056/aba9bb

Exploration and elaboration of photo-induced proton transfer dynamical mechanism for novel 2-[1,3]dithian-2-yl-6-(7aH-indol-2-yl)-phenol sensor

Lei Xu(许磊), Tian-Jie Zhang(张天杰), Qiao-Li Zhang(张巧丽), Da-Peng Yang(杨大鹏)

Chin. Phys. B, 2020, 29 (**5**): 053102. DOI: 10.1088/1674-1056/ab8208

Re effects in model Ni-based superalloys investigated with first-principles calculations and atom probe tomography

Dianwu Wang(王殿武), Chongyu Wang(王崇愚), Tao Yu(于涛), Wenqing Liu(刘文庆)

Chin. Phys. B, 2020, 29 (**4**): 043103. DOI: 10.1088/1674-1056/ab6587

The substituent effect on the excited state intramolecular proton transfer of 3-hydroxychromone

Yuzhi Song(宋玉志), Songsong Liu(刘松松), Jiajun Lu(陆佳骏), Hui Zhang(张慧), Changzhe Zhang(张常哲), Jun Du(杜军)

Chin. Phys. B, 2019, 28 (**9**): 093102. DOI: 10.1088/1674-1056/ab3434

Study on the electromagnetic propertiesof a coated radar absorbent

Zhang Shuan-Qin

Chin. Phys. B, 2012, 21 (**6**): 065101. DOI: 10.1088/1674-1056/21/6/065101

Electronic shell study of prolate Li_n ($n = 15$–17) clusters: Magnetic superatomic molecules*

Lijuan Yan(闫丽娟)†, Jianmei Shao(邵健梅), and Yongqiang Li(李永强)‡

College of Electronics & Information Engineering, Guangdong Ocean University, Zhanjiang 524088, *China*

(Received 3 August 2020; revised manuscript received 25 August 2020; accepted manuscript online 9 September 2020)

The non-spherical lowest-lying Li_n ($n = 15$–17) isomers were found with high symmetric compact structures, of which the stability was not rationalized in a previous report (*J. Chem. Phys.* **119** 9444 (2003)). Based on the newly proposed super-valence bond model, the three prolate lithium clusters can be viewed as magnetic superatomic molecules, which are composed by sharing valence electron pairs and nuclei between two superatom units, namely, Li_{10} or Li_{11}, and thus their stability can be given a good understanding. Molecular orbital and chemical bonding analysis clearly reveal that the Li_n ($n = 15$–17) clusters with prolate shapes are magnetic superatomic molecules. Our work may aid in the developments of the cluster-assembled materials or superatom-bonds.

Keywords: jellium model, geometry and electronic shells, magnetic properties, stability, electron delocalization

PACS: 51.60.+a, 31.15.ae, 31.15.A–, 31.15.xw **DOI:** 10.1088/1674-1056/abb669

1. Introduction

One of the interesting issues in cluster science is to investigate the stability and structures of atomic clusters, which is important for both fundamental science and applications. In theory, many efforts have been made to comprehend the stability of atomic clusters, for instance, the valence-electron counting rules (including octet rule, 18-electron rule, and Wade–Mingos counting rule),[1–4] the polyhedral skeletal electron pair theory (PSEPT),[5] aromaticity,[6] the tensor surface harmonic model (TSHM),[7] the jellium model,[8–11] the grand unified model,[12] and so on. For the small metal clusters, their stability can be well described by using the jellium model.[8–11] In this model, the ionic charge of the cluster's atomic nuclei and the innermost electrons are replaced by a uniform positive spherical external potential, wherein the movements of valence electrons are subjected. For the common square well potential, the effective valence electronic filling order in a metal cluster is $|1S^2|1P^6|1D^{10}|2S^21F^{14}|2P^6|1G^{18}|2D^{10}3S^21H^{22}|\cdots$, with S–P–D–F–G–H denoting the angular momentum characters and the electronic shell closures associating to the magic clusters.

Stemming from the jellium model, the concept of superatoms was introduced to interpret the mass spectra of sodium clusters, where the high peaks of $N = 8$, 20, 40, 58, and 92 had been identified to the electronic shell closure.[9] The electronic states in a superatom were accommodated into shells with the valence electronic spectrums and chemical behaviour resembling to the situation of atoms. In year 2008, Walter and coworkers further extended the superatom concept to illustrate the stability of ligand-protected gold nanoparticles, such as $Au_{102}(SR)_{44}$, $Au_{39}(PR_3)_{14}X_6$, $Au_{11}(PR_3)_7X_3$, and $Au_{13}(PR_3)_{10}X_{23}$ protected by thiolate (SR) or phosphine and halide (PR_3, X) ligands, of which the high stability of the spherical core are largely due to their closed electronic shells.[13] The superatom concept had been successfully applied to understand the stability of many pure metal clusters and ligand-protected nanoclusters with spherical shapes.[9,13–18] As for the non-spherical clusters, Clemenger had suggested an ellipsoidal shell model, which achieved success in many cases by tuning the two parameters (δ, U) to fit their energy-level splittings.[19] However, the introduced parameters can not give direct physical picture, and the model is entirely structureless.

Taking Li_{14}, Li_{10}, and Li_8 clusters as examples, Cheng and Yang proposed the super valence bond (SVB) model, of which superatoms can share both valence electron pairs and nuclei for shell closure.[20] In other words, the stability of a non-spherical metallic cluster can be understood from its shell closure molecule, which is formed via super bonding between superatoms and superatoms or other atoms. Therefore, the superatom maybe a whole unit, or fused with other units in the studied systems. To date, three bonding modes have been revealed, including a vertex-sharing, a face-sharing and non-sharing modes. According to the SVB model, the stability of $Au_{38}(SR)_{24}$ and $[Au_{20}(PPhy_2)_{10}Cl_4]Cl_2$ have be rationalized, where the stable Au_{23}^{9+} and Au_{20}^{6+} cores are respectively proved as 23c–14e bi-icosahedral[21] and 20c–14e incomplete

*Project supported by the PhD Starting Fund of Guangdong Ocean University (Grant No. 120702/R17077) and the National Natural Science Foundation of China (Grant No. 11704080).

†Corresponding author. E-mail: ylj_gdou@126.com

‡Corresponding author. E-mail: lyq196399@163.com

© 2020 Chinese Physical Society and IOP Publishing Ltd

bi-icosahedral superatomic molecules.[22] The SVB model has given good understanding of the electronic stability of some non-spherical pure metal clusters and some elongated ligand-protected gold clusters.[20–27]

In this work, the stability of the lowest-energy Li_n clusters within the range of $n = 15$–17 is explained in detail on the basis of SVB model. Their prolate geometric structures are firstly relocated based on the particle swarm optimisation algorithm (PSO) search and density-functional theory (DFT) calculations. Then, the relative stability of the lowest-energy isomers is discussed. From the aspects of geometric structures and electronic shells, the properties of superatomic molecules in Li_n ($n = 15$–17) are analyzed, of which the open electronic shells grant them well-defined magnetic moments maybe offering potential applications in electronic devices.

2. Computational details

The low energy isomers of Li_n ($n = 15$–17) clusters are obtained by the PSO algorithm implemented in Crystal structure AnaLYsis by Particle Swarm Optimization (CALYPSO) package[28] interfaced with Gaussian, which is an efficient method for the stable or metastable cluster structure prediction. For the initial generation, its structures are randomly produced, while 60% structures of the other generations are derived from previous generations, evolved by PSO and 40% are new, generated randomly. Each generation contains 50 structures. The search convergence has been achieved by 50 generations of structural candidates completed. Low-lying structures with the energy difference less than 2 eV from the global minimum isomer are re-optimized at the DFT calculations of Gaussian 16 code.[29] The frequency calculations identify these picked low energy isomers as true local minima due to without any virtual values. The spin states for each isomer are also considered. With the variation of multiplicities for the same structure, the multiplicity of the lowest energy isomer is designated as the ground state. In order to give reasonable results, three functionals (pure functional PW91,[30] meta-GGA functional M06-L,[31] and hybrid functional TPSSH[32]) are adopted, which are proved most valid for the lithium cluster systems. SDD is chosen as the basis set.[33] All the visualizations are completed by using Multiwfn_3.6.[34]

3. Results and discussion

The first five low energy geometric structures of the Li_n ($n = 15$–17) clusters are displayed in Fig. 1, labeled as $n.X$, where n denotes the number of Li atoms in the range of 15 to 17, and X is A, B, C, D, E corresponding to the several low-lying isomers arranged by their increasing relative energy. At the calculations of M06L/SDD level, their symmetries and relative energies are shown with the cartesian coordinates offered in SI. To give a clear view of the lowest-energy structures, all the chosen orientations of Li_n ($n = 15$–17) isomers in this paper is easy to distinguish the molecular structures and their corresponding two monomers. The lowest energy isomer of Li_{15} is a capped double centered square antiprism with the C_{2v} symmetry, of which the ground state is dual. For Li_{16} and Li_{17},

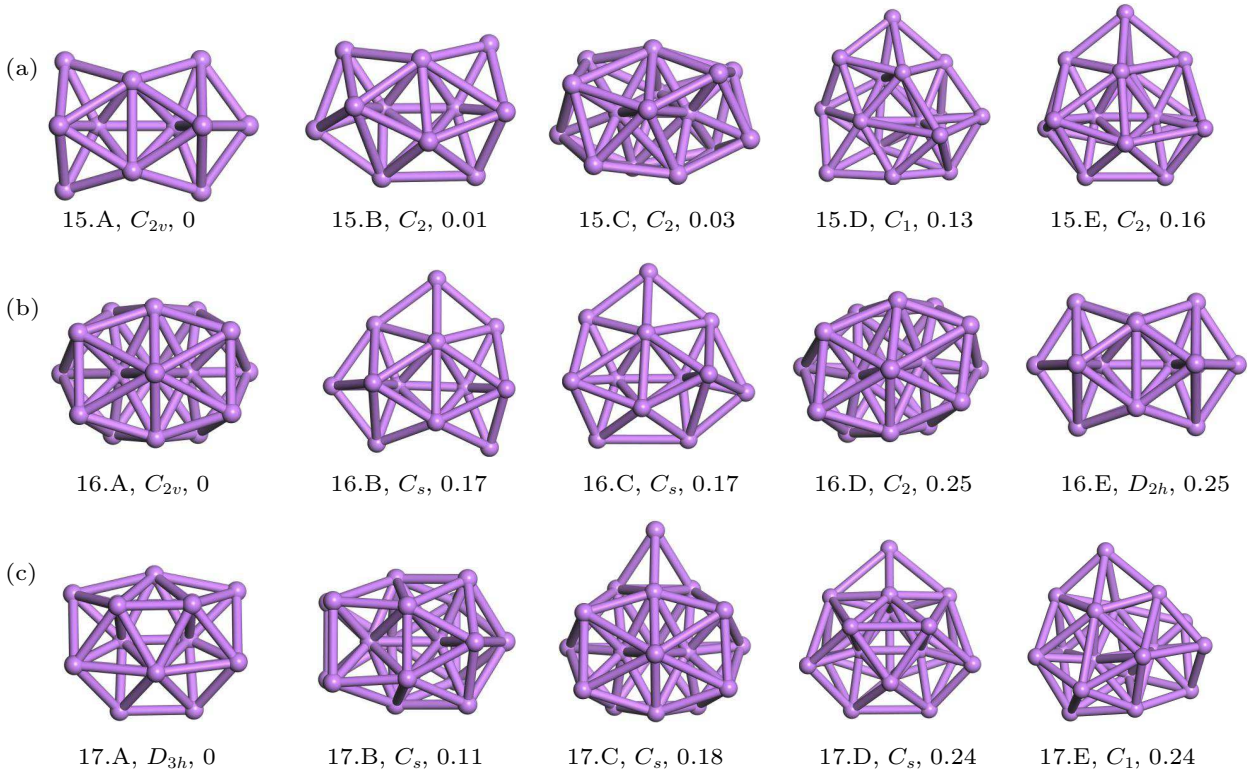


Fig. 1. The first five low-energy isomers of (a) Li_{15}, (b) Li_{16}, and (c) Li_{17} (unit: eV). * 16.E has an imaginary frequency of −47.45 with the relaxation to 16.A.

the most stable structures are distorted capped icosahedron and double tricapped centered trigonal prism with C_{2v} and D_{3h} symmetries, of which the total magnetic moments are 2 μ_B and 3 μ_B, respectively. Our predicted structures are in excellent accordance with the results of Fournier and co-workers, where a global optimization algorithm of the Tabu Search algorithm in Descriptor Space is adopted to search possible low-energy isomers,[35] while the stability of Li_n (n = 15–17) is not given due to the prolate shapes and open electronic shells.

As a starting point for theoretical understanding of the stability of the lowest energy Li_n (n = 15–17) clusters with the non-spherical shapes, the average binding energy (E_b) per atom and the fragmentation energy (E_f) are calculated respectively using the following formulas:

$$E_b(Li_n) = \frac{nE(Li) - E(Li_n)}{n},$$
$$E_f(Li_n) = E(Li_{n-1}) + E(Li) - E(Li_n).$$

In the above equations, the value of n is from 15 to 17, representing the cluster sizes. $E(Li_n)$ and $E(Li_{n-1})$ denote the total energy of the Li_n clusters and the fragment Li_{n-1}, of which the formation is one lithium atom detached from its parent cluster Li_n. $E(Li)$ is the total energy of the free state Li atom.

The corresponding theoretical results are given in Table 1. It can be seen that the variation trends of E_b and E_f produced by the three functionals are coincident for the ground state structures of Li_n (n = 15–17), where E_b increases monotonically with their sizes and the gain in energy of E_f is to rise first and then a drop going from Li_{15} to Li_{17}. However, the results calculated by M06L functional are more reliable due to the obtained ionization potentials outperforming that of local big basis used by Fournier *et al.*[35] and closer to the experimental values.[36] Moreover, E_f can be used to measured the dissociation, where a large positive value predicts to dissociate difficultly. Noteably, the E_f of Li_{16} is largest among the three global minimum isomers, indicating its relative high stability.

The energy gap (E_{gap}), defined as the energy difference of the highest occupied molecular orbital (HOMO) and the lowest unoccupied molecular orbital (LUMO), is also examined for a cluster with a large HOMO–LUMO gap can enhance its stability. At the M06L/SDD calculations, the HOMO–LUMO gaps of aspherical Li_n (n = 15–17) clusters are 0.30, 0.40, and 0.70 eV, respectively, much smaller than that of the renowned superatoms, for instance Al_{13}^- (1.87 eV)[37] and C_{60} (1.72 eV).[38] However, their gaps are moderate compared with the gaps of typical magnetic superatoms, such as VNa_8 (0.69 eV),[39] $MnSr_9$ (0.35 eV),[40] $FeMg_8$ (0.64 eV),[41] $MnMg_8$ (0.35 eV),[41] pure metal superatoms Cs_{13} (0.21 eV),[42] and Na_{55}^+ (0.27 eV),[43] *etc*.

Aiming for the comprehending of their stability, we focus on the roles of geometric and electronic shells, which are important for the stability and properties of small clusters.[44,45] Obviously, the most stable isomers for the three clusters all have the cage-like shapes centered by two lithium atoms, and such closed geometric structures will enhance their stability. According to the SVB model, the non-spherical Li_n (n = 15–17) structures can be viewed as an assembly of two centered superatoms. As shown in Fig. 2, the Li_{15} cluster can be formed by the fusion of a capped centered square antiprism (Li_{10}) and a double capped centered square antiprism (Li_{11}), where the two building units share the middle six lithium atoms. The Li_{16} and Li_{17} clusters are assembled by the same building unit (Li_{11}) with the middle six or five lithium atoms shared, respectively. Compared to Li_{15}, the Li_{11} unit is distorted in Li_{16} or a slight elongation for Li_{17}. Besides, the most stable isomers of Li_{17} have a close relation to the lowest-energy structure of Li_{16} as mentioned in previous work.[35] Along the direction of perpendicular to axis, if a pair of middle equivalent lithium atoms of Li_{17} are replaced by a single lithium atom at their average position, the lowest-lying Li_{16} will be obtained. The resembled assembly styles indicate that the three clusters should possess many similar characters. In respect of geometric structures, we intuitively infer that the non-spherical Li_n (n = 15–17) clusters can be regarded as superatomic molecules.

Table 1. The symmetry, the fragmentation energy (E_f), the binding energy (E_b) per atom, the energy gaps (E_{gap}), the vertical ionization potential, the valence electrons (ve), the electron configuration, and the total magnetic moment (μ, in units of μ_B) of magnetic superatomic molecules Li_{15}, Li_{16}, and Li_{17}.

Li_n	Methods	Symmetry	E_f	E_b	E_{gap}	vip	ve	Electron configuration	μ
Li_{15}	PW91	C_{2v}	1.30	1.09	0.28	3.85	15	$(\sigma_{1S})^2(\sigma^*_{1S})^2(\pi_{1P_x,1P_y})^4(\sigma_{1P_z})^2(\pi^*_{1P_x,1P_y})^4$ $(\delta_{1D_{x2-y2}})^1_\alpha(\sigma_{2S})^0_\alpha(\delta_{1D_{xy}})^0_\alpha(\sigma_{2S})^0_\beta(\delta_{1D_{x2-y2,xy}})^0_\beta$	1
	M06L		1.35	1.18	0.30	3.62			
	TPSSH		1.29	1.09	0.78	3.78			
Li_{16}	PW91	C_{2v}	1.47	1.11	0.44	4.16	16	$(\sigma_{1S})^2(\sigma^*_{1S})^2(\pi_{1P_x,1P_y})^4(\sigma_{1P_z})^2(\pi^*_{1P_x,1P_y})^4$ $(\delta_{1D_{x2-y2,xy}})^2_\alpha(\sigma_{2S})^0_\alpha(\delta_{1D_{x2-y2,xy}})^0_\beta(\sigma_{2S})^0_\beta$	2
	M06L		1.58	1.20	0.40	3.92			
	TPSSH		1.45	1.11	0.85	4.09			
Li_{17}	PW91	D_{3h}	1.42	1.13	0.57	4.00	17	$(\sigma_{1S})^2(\sigma^*_{1S})^2(\pi_{1P_x,1P_y})^4(\sigma_{1P_z})^2(\pi^*_{1P_x,1P_y})^4$ $(\delta_{1D_{x2-y2,xy}})^2_\alpha(\sigma_{2S})^1_\alpha(\delta_{1D_{x2-y2,xy}})^0_\beta(\sigma_{2S})^0_\beta$	3
	M06L		1.54	1.22	0.70	3.87			
	TPSSH		1.38	1.12	0.90	3.92			

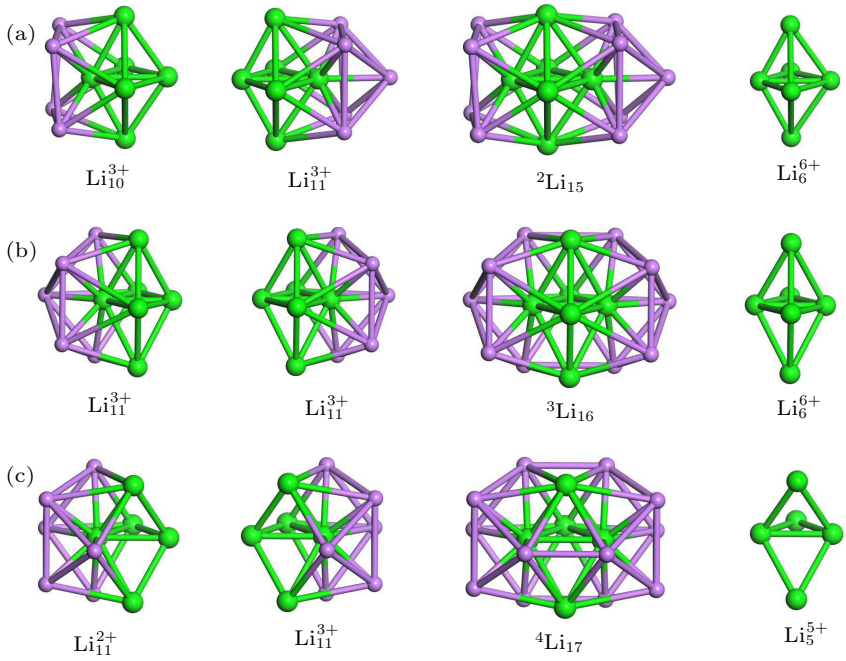


Fig. 2. Diagrams of di-superatomic model for the prolate lithium clusters (a) Li_{15}, (b) Li_{16}, and (c) Li_{17}.

To identify our supposition, the electronic stability of Li_n (n = 15–17) clusters is analyzed from the aspects of their canonical Kohn–Sham molecular orbitals (MOs) and chemical bonding patterns. The MOs diagrams of Li_{15} cluster are shown in Fig. 3. The lowest two sets MOs (σ_{1S} and σ^*_{1S}) are composed of two 1S superatomic orbitals (SAOs). Due to the effects of its prolate geometric structure, the next two doubly degenerate sets MOs (π_{1P_x,P_y} and $\pi^*_{1P_x,P_y}$), which are derived from four $1P_x$ and $1P_y$ SAOs, are broken into different energy levels with the energy splitting of 0.11 eV at the M06L/SDD calculation. The next two sets (σ_{1P_z} and $\sigma^*_{1P_z}$) are formed by two $1P_z$ SAOs. The non-spherical shape of also broke the degeneracy of the $\delta_{1D_{x2-y2,xy}}$ MOs, where $\delta_{1D_{xy}}$ of α is pushed 0.36 eV higher in energy calculated by M06L/SDD. Hence, the corresponding valence electronic configuration of the Li_{15} cluster is $(\sigma_{1S})^2(\sigma^*_{1S})^2(\pi_{1P_x,1P_y})^4$ $(\sigma_{1P_z})^2(\pi^*_{1P_x,1P_y})^4$ $(\delta_{1D_{x2-y2}})^1_\alpha(\sigma_{2S})^0_\alpha(\delta_{1D_{xy}})^0_\alpha(\sigma_{2S})^0_\beta(\delta_{1D_{x2-y2,xy}})^0_\beta$, of which the HOMO-LUMO gap (0.78 eV/TPSSH) is formed by the energy difference between $(\delta_{1D_{x2-y2}})\alpha$ and $(\sigma_{1S})\alpha$. The total magnetic moment of Li_{15} is 1 $\mu_B$due to one unpaired electron.

As for the Li_{16} and Li_{17} clusters, their MOs have a great degree of similarity to that of Li_{15} cluster except for the degenerate MOs with a different energy splitting, especially for $\delta_{1D_{x2-y2,xy}}$, of which both the shapes and orders change a lot. As shown in Fig. 3, the effective valence electronic configurations of Li_{16} and Li_{17} clusters are $(\sigma_{1S})^2(\sigma^*_{1S})^2(\pi_{1P_x,1P_y})^4(\sigma_{1P_z})^2(\pi^*_{1P_x,1P_y})^4$ $(\delta_{1D_{x2-y2,xy}})^2_\alpha(\sigma_{2S})^0_\alpha$ $(\delta_{1D_{x2-y2,xy}})^0_\beta(\sigma_{2S})^0_\beta$ and $(\sigma_{1S})^2(\sigma^*_{1S})^2(\pi_{1P_x,1P_y})^4(\sigma_{1P_z})^2(\pi^*_{1P_x,1P_y})^4$ $(\delta_{1D_{x2-y2,xy}})^2_\alpha$ $(\sigma_{2S})^1_\alpha(\delta_{1D_{x2-y2,xy}})^0_\beta(\sigma_{2S})^0_\beta$, respectively. The number of unpaired electrons for the Li_{16} and Li_{17} clusters is 2 and 3, thus with the total magnetic moment of 2 and 3 μ_B, respectively. The HOMO–LUMO gap of Li_{16} cluster is 0.85 eV (TPSSH/SDD) formed by the energy difference between $(\delta_{1D_{x2-y2,xy}})\alpha$ and $(\sigma_{2S})\alpha$, whereas $(\sigma_{1P_z}))^*_\alpha$-$(\sigma_{2S})\alpha$ is the HOMO–LUMO gap of Li_{17} cluster (0.90 eV, TPSSH/SDD). From the MOs analysis, the molecular properties of non-spherical Li_n (n = 15–17) clusters are pretty obvious.

To further verify the existence of superatom–superatom bonds in the prolate Li_n (n = 15–17) clusters, we present a vivid view on their chemical bonding patterns, which are obtained by adaptive natural density partitioning (AdNDP) of a chemical bonding analysis tool.[46] As figure 4 shows, the Li_{15} cluster possesses one 15c–2e super-σ-bond over the whole cluster and three super lone pair (LP) orbitals, namely, S, P_x, and P_y, which belongs to each superatom Li_{10}^{3+} and Li_{11}^{3+}. The remaining one is a single electron, forming the magnetic moments of Li_{15}. The bond patterns of Li_{16} and Li_{17} are similar to Li_{15}, both of them have one super-σ-bond and three LP orbitals. Besides, the number of single electron is two for Li_{16}, which are filled in the bonding MOs $\delta_{1D_{x2-y2,xy}}$ of α. As for Li_{17}, the remaining three single electrons occupy the bonding MOs $\delta_{1D_{x2-y2,xy}}$ and σ_{2S} of α. Thus, the super bond orders for Li_{15}, Li_{16}, and Li_{17} are 1.5, 2.0, and 2.5, respectively. Such a superatomic bonding pattern has been found in other superatomic molecules, for instance, 26e $Li_{20}Mg_3$,[24] 30e $Li_{18}Mg_3Al$,[24] and face-sharing bitetrahexahedral M_1M_2@Li_{20} (M_1/M_2 = Ti and W).[23] Corresponding, the occupancy numbers (ON) of super LPs and super-σ-bond for Li_{15}, Li_{16}, and Li_{17} are relatively high with ON = 1.90–2.00 $|e|$. By the chemical bonding analysis, the bonding patterns of non-spherical Li_n (n = 15–17) exhibit the behavior of magnetic superatomic molecules in a straightforward manner.

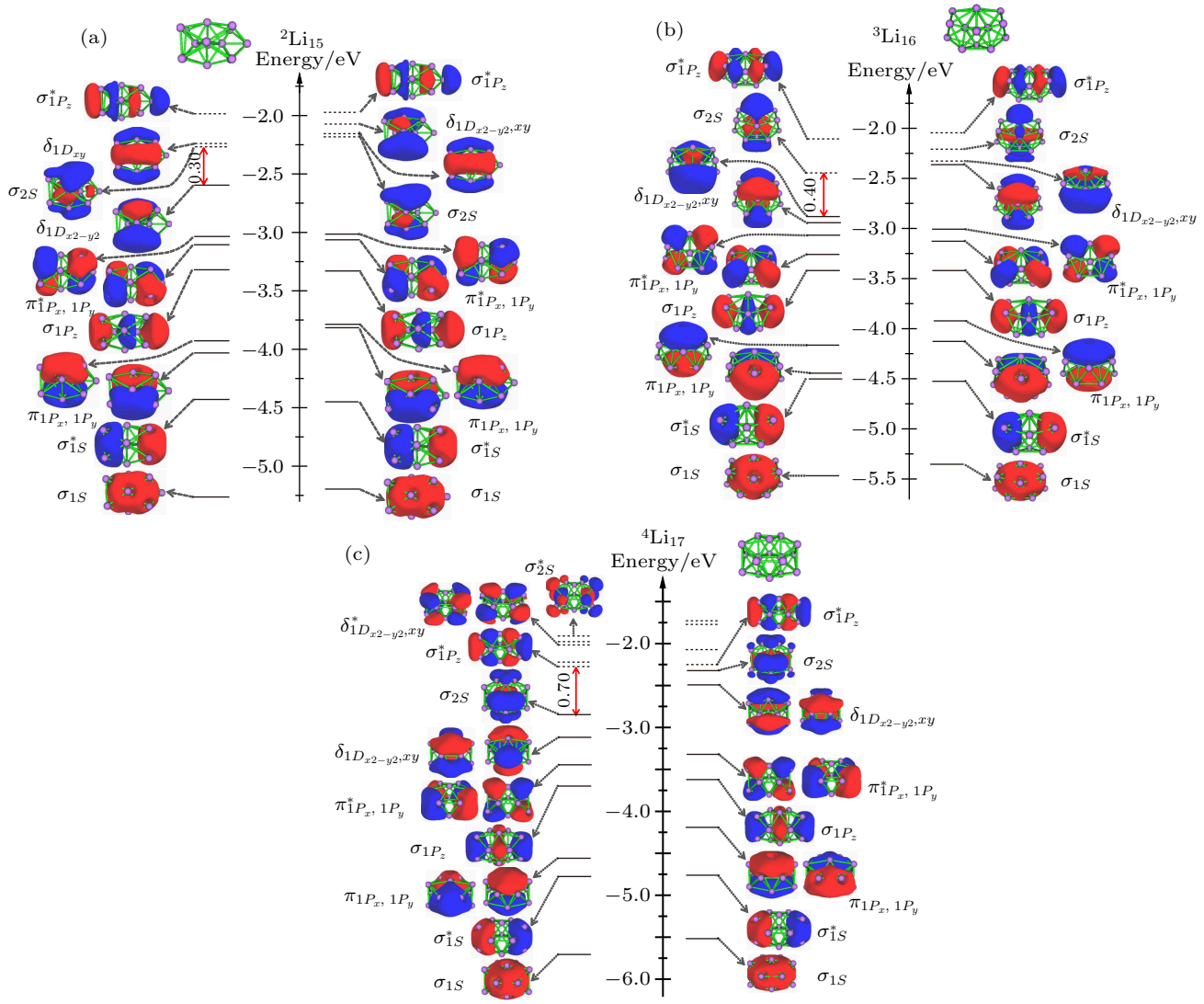


Fig. 3. The Kohn–Sham MOs diagrams of magnetic superatomic molecules: (a) Li_{15}, (b) Li_{16}, and (c) Li_{17}. The continuous lines and dotted lines correspond to the occupied or unoccupied levels, respectively, where the energy states in a horizontal line denotes degenerated. The energy gaps are marked with double arrow red lines (unit: eV).

Based on above analysis, the prolate Li_n ($n = 15$–17) clusters are identified as magnetic superatomic molecules considering their geometric structures and electronic shells. Also, their stability can be rationalized according to the ellipsoidal shell model, where the modified spherical potentials cause the degenerate electronic states undergoing splitting. Therefore, the corresponding valence electronic filling orders are $1S^21P^61D^4_\alpha 1D^3_\beta$, $1S^21P^61D^5_\alpha 1D^3_\beta$, $1S^21P^61D^5_\alpha 1D^3_\beta 2S^1_\alpha$, successively, of which the MOs are supplemented in SI. This situation is to be expected for their geometric structures are not deviated far from the spherical shapes and composed by a linear combinations of cluster units. Actually, many superatomic molecules can be analyzed from the views of ellipsoidal shell model due to both models rooted in the jellium model, whereas the super hybrid bonds of Au_{20} or the nanoclusters assembled from more than two clusters are beyond the scope of the ellipsoidal shell model. To enhance the molecular properties of our studied clusters, the two central lithium atoms can be replaced by transition metal atoms Co, with the geometric structures and the spin states unchanged, which are found as the lowest-lying isomers for Co_2Li_n ($n = 13$–15).

From Li_{15} to Li_{17} clusters, with the increasement of lithium atoms, the new lowest-lying isomers tend to be more compact and symmetric geometric structures, and thus the charge distribution over the surface becomes more even. At the same time, the shapes of degenerate MOs are more symmetrical, and their separated degenerate energy level will be merged. Despite possessing open electronic shells for Li_n ($n = 15$–17), the stability is granted by their properties of magnetic superatomic molecules. The moderated HOMO–LUMO gaps and closed geometric structures further enhance their stability. In addition, the magnetic superatomic molecules Li_{17} has 17 effective valance electrons, and then its assembled unit possesses multiple valence (Li^{3+}_{11} and Li^{2+}_{11}).

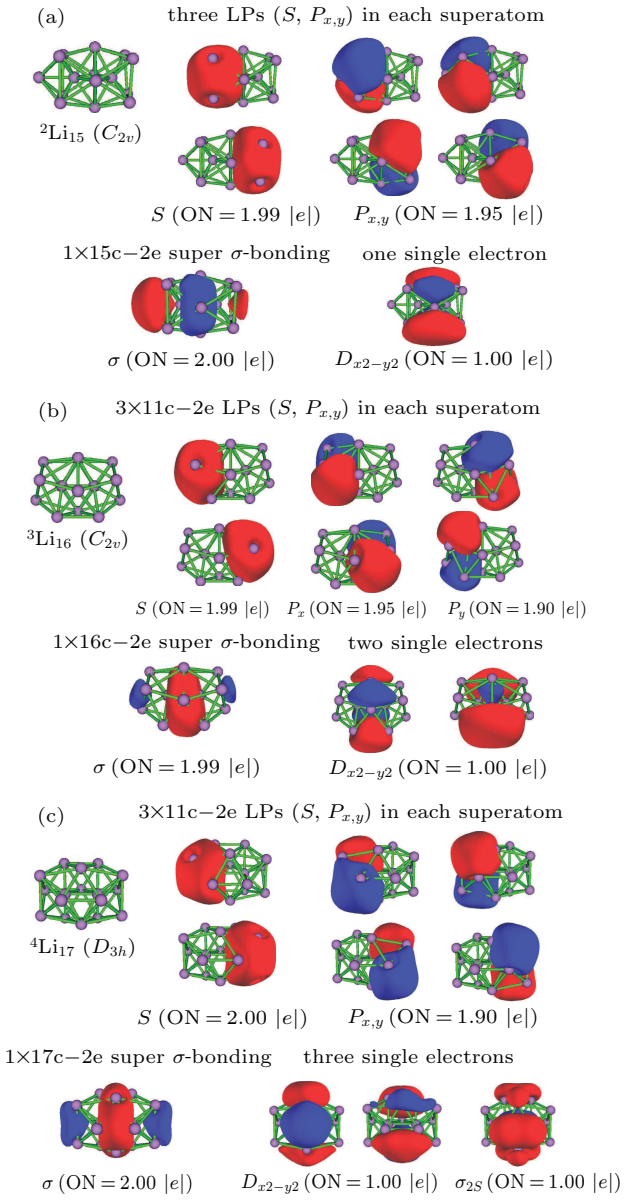


Fig. 4. AdNDP localized natural bonding orbitals of magnetic superatomic molecules: (a) Li_{15}, (b) Li_{16}, and (c) Li_{17}.

4. Conclusions

To summary, we present a novel understanding of the stability of prolate Li_n (n = 15–17) clusters based on the SVB model. By the PSO algorithm, the shapes of two lithium atoms centered in Li_n cages are relocated in good agreement with the previous report. Frequency calculations also confirm that they are as true local minima. Energy calculations predict that the three non-spherical lithium clusters are very stable, and their moderate HOMO–LUMO gaps will further enhance the stability. According to the SVB model, the three prolate lithium clusters can be regarded as magnetic superatomic molecules. With a six-nuclei octahedron shared, the assembly of 10c–7e and 11c–8e or two 11c–8e units can respectively obtain the most stable Li_{15} and Li_{16}, where Li_{17} are assembled by the fusion of 11c–8e and 11c–9e units shared with a five-nuclei bi-tetrahedron. MOs analysis and chemical bonding patterns reveal that they all possess the properties of magnetic superatomic molecules and the total magnetic moments are 1, 2, and 3 μ_B, respectively. The SVB model gives a new physical insight of the stability of the prolate Li_n (n = 15–17) clusters, where their open electronic shells further manifest the universality of the SVB model for the non-spherical clusters.

Acknowledgment

We thank the discussion with Dr. Liren Liu.

References

[1] Lewis G N 1916 *J. Am. Chem. Soc.* **38** 762
[2] Langmuir I 1921 *Science* **54** 59
[3] Sidgwick N V and Bailey R W 1934 *Proc. Roy. Soc. Lond. A* **144** 521
[4] Mingos D M P 1976 *J. Chem. Soc. Dalton Trans.* **7** 1163
[5] Wade K 1971 *J. Chem. Soc. D* **15** 792
[6] Randic M 1977 *J. Am. Chem. Soc.* **99** 444
[7] Stone A J 1981 *Inorg. Chem.* **20** 563
[8] Ekardt W 1984 *Phys. Rev. B* **29** 1558
[9] Knight W D, Clemenger K, de Heer W A, Saunders W A, Chou M Y and Cohen M L 1984 *Phys. Rev. Lett.* **52** 2141
[10] Brack M 1993 *Rev. Mod. Phys.* **65** 677
[11] de Heer W A 1993 *Rev. Mod. Phys.* **65** 611
[12] Xu W W, Zhu B, Zeng X C and Gao Y 2016 *Nat. Commun.* **7** 13574
[13] Walter M, Akola J, Lopez-Acevedo O, Jadzinsky P D, Calero G, Ackerson C J, Whetten R L, Grönbeck H and Häkkinen H 2008 *Proc. Natl. Acad. Sci. USA* **105** 9157
[14] Zhu M, Aikens C M, Hollander F J, Schatz G C and Jin R 2008 *J. Am. Chem. Soc.* **130** 5883
[15] Jiang D E, Whetten R L, Luo W and Dai S 2009 *J. Phys. Chem. C* **113** 17291
[16] Xie J, Zheng Y and Ying J Y 2009 *J. Am. Chem. Soc.* **131** 888
[17] Jiang D E, Walter M and Akola J 2010 *J. Phys. Chem. C* **114** 15883
[18] Hakkinen H 2012 *Nat. Chem.* **4** 443
[19] Clemenger K 1985 *Phys. Rev. B* **32** 1359
[20] Cheng L and Yang J 2013 *J. Chem. Phys.* **138** 141101
[21] Cheng L, Ren C, Zhang X and Yang J 2013 *Nanoscale* **5** 1475
[22] Yuan Y, Cheng L and Yang J 2013 *J. Phys. Chem. C* **117** 13276
[23] Yan L 2019 *J. Phys. Chem. A* **123** 5517
[24] Wang H and Cheng L 2017 *Nanoscale* **9** 13209
[25] Liu L, Li P, Yuan L F, Cheng L and Yang J 2016 *Nanoscale* **8** 12787
[26] Yan L, Cheng L and Yang J 2015 *Chin. J. Chem. Phys.* **28** 476
[27] Yan L, Cheng L and Yang J 2015 *J. Phys. Chem. C* **119** 23274
[28] Lv J, Wang Y, Zhu L and Ma Y 2012 *J. Chem. Phys.* **137** 084104
[29] Frisch M J, Trucks G W, Schlegel H B, Scuseria G E, Robb M A, Cheeseman J R, Scalmani G, Barone V, Mennucci B, Petersson G A, *et al.* 2016 *Gaussian* 16, *Revision B.*01, *Gaussian, Inc.: Wallingford, Ct.*
[30] Perdew J P and Wang Y 1992 *Phys. Rev. B* **45** 13244
[31] Zhao Y and Truhlar D G 2006 *J. Chem. Phys.* **125** 194101
[32] Grimme S, Antony J, Ehrlich S and Krieg H 2010 *J. Chem. Phys.* **132** 154104
[33] Hay P J and Wadt W R 1985 *J. Chem. Phys.* **82** 270
[34] Lu T and Chen F 2012 *J. Comput. Chem.* **33** 580
[35] Fournier R, Cheng J B Y and Wong A 2003 *J. Chem. Phys.* **119** 9444
[36] Dugourd P, Rayane D, Labastie P, Vezin B, Chevaleyre J and Broyer A M 1992 *Chem. Phys. Lett.* **197** 433
[37] Khanna S N, Rao B K and Jena P 2002 *Phys. Rev. B* **65**
[38] Gong X G and Zheng Q Q 1995 *Phys. Rev. B* **52** 4756
[39] Zhang X, Wang Y, Wang H, Lim A, Gantefoer G, Bowen K H, Reveles J U and Khanna S N 2013 *J. Am. Chem. Soc.* **135** 4856
[40] Pradhan K, Reveles J U, Sen P and Khanna S N 2010 *J. Chem. Phys.* **132** 124302
[41] Medel V M, Reveles J U, Khanna S N, Chauhan V, Sen P and Castleman A W 2011 *Proc. Natl. Acad. Sci. USA* **108** 10062
[42] Aguado A 2012 *J. Phys. Chem. C* **116** 6841
[43] Vasquez-Perez J M, Gamboa G U, Mejia-Rodriguez D, Alvarez-Ibarra A, Geudtner G, Calaminici P and Koster A M 2015 *J. Phys. Chem. Lett.* **6** 4646
[44] Reber A C and Khanna S N 2017 *Acc. Chem. Res.* **50** 255
[45] Luo Z and Castleman A W 2014 *Acc. Chem. Res.* **47** 2931
[46] Zubarev D Y and Boldyrev A I 2008 *Phys. Chem. Chem. Phys.* **10** 5207